RSC Advances

ROYAL SOCIETY OF CHEMISTRY

www.rsc.org/advances

Journal Name

ARTICLE

Naphthalene Diimide and Benzothiadiazole Copolymer Acceptor for All-Polymer Solar Cells with improved Open-Circuit Voltage and Morphology

Received 00th January 20xx,
Accepted 00th January 20xx

DOI: 10.1039/x0xx00000x

www.rsc.org/

Fangbin Liu[a,b], Hui Li[a,b], Yishi Wu[a], Chunling Gu*[a] and Hongbing Fu*[a]

Donor-acceptor (D-A) copolymers PNDIBTH and PNDIBTOC8 based on two strong electron-deficient units, naphthalene diimide and benzothiadiazole, were synthesized and used as acceptor for the fabrication of all-polymer solar cells (all-PSCs). Introduction of the two octyloxy side chains onto the benzothiadiazole in PNDIBTOC8 could not only increase the solubility and molecular weight of polymer, but also alter its optical and electronic properties. Compared with PNDIBTH, PNDIBTOC8 possesses much higher molecular weight and raised LUMO level up to -3.72 eV. Investigation of the photovoltaic performance of two polymers in all-PSCs using polymer PBDTTT-C-T as donor materials indicated that PNDIBTOC8 provides excelllent power conversion efficiency (PCE) of 3.14% with high open-circuit voltage (V_{oc}) of 0.90 V, much higher than that of PNDIBTH-based device (PCE of 1.20% with V_{oc} of 0.76 V). Moreover, the dendrite-like phase separation in PNDIBTOC8-based blend film contributes to the high and more-balanced charge mobilities.

Introduction

Solution-processed bulk heterojunction (BHJ) organic solar cells (OSCs) have attracted great attention as alternative photon harvesting devices because of their tunable optical and electronic properties, light weight, mechanical flexibility, and potential for high-throughput manufacture[1-4]. Over the last decades, OSCs have made great strides and power conversion efficiencies (PCEs) over 10% has been achieved in recent publications.[5] Generally, record efficiencies directly result from the development of new conjugated materials[6-9], especially for donors, which mixed with a fullerene derivative such as [6,6]-phenyl-C61-butyric acid methyl ester ($PC_{61}BM$) or [6,6]-phenyl-C71-butyric acid methyl ester ($PC_{71}BM$) as electron-accepting components in BHJ blends. Despite the attraction of fullerenes in OSCs, they face limitations such as: a) costly synthesis with high purity; b) unfavourable optical absorption characteristics at the long wavelength; and c) limited chemical and energetic tunability.[10-11] In comparison to fullerene-based OSCs, all-polymer active layers offer unique attractions owing to the chemical and electronic tunability of the donor and acceptor polymers, suggesting intriguing opportunities for enhancing PCE.[12-13] Currently, all-polymer solar cells (all-PSCs) have shown PCEs of 3.3-6.3%.[14-19] However, the development of polymer acceptors is still at the infant stage relative to fullerenes and more novel polymer acceptors should be explored urgently.

Naphthalene diimide (NDI) units are widely used for constructing n-type organic semiconductors due to its highly electron-deficient character. The NDI-based copolymers are one of the most promising classes of polymer acceptor materials, and have shown some of the highest power conversion efficiencies recorded in all-PSCs.[15-21] Notably NDI-thiophene and NDI-selenophene copolymer acceptors achieved the high PCEs of 5.7% and 4.8%, with high electron mobilities of 3.6×10^{-4} and 2.6×10^{-4} cm^2 V^{-1} s^{-1} in blend film, respectively.[15-16] However, a common feature of NDI-based copolymer used in all-PSCs is the deep lowest unoccupied molecular orbital (LUMO) level, typically in the range of -3.9 - -4.3 eV[22-27], which creates a small difference between the LUMO level of acceptor and the highest occupied molecular orbital (HOMO) level of donor. To the best of our knowledge, most works with NDI-based copolymers as acceptor materials produce a moderate V_{oc} of less than 0.80 eV, which is greatly due to their deep LUMO level.[20, 26-29] Therefore, raising the LUMO level of acceptor would be an efficient strategy to achieve high V_{oc} and allow making more efficient all-PSCs.

Attaching an electron-donating or electron-withdrawing group to main chain has been largely considered to optimize the HOMO/LUMO levels of conjugated polymers and the V_{oc} of the corresponding PSCs.[30-34] In the case of designing polymer, alkoxy group can not only increase the solubility of polymer, but also elevate the LUMO/HOMO levels of copolymer due to the electron-donating property of alkoxy side chain. This is bad for donor polymer applied in PSCs with decreased V_{oc}. For

[a] Beijing National Laboratory for Molecular Sciences, Key Laboratory of Photochemistry, Institute of Chemistry, Chinese Academy of Sciences, Beijing, 100190, P. R. China. hongbing.fu@iccas.ac.cn, chunlgu@iccas.ac.cn.
[b] University Chinese Academy of Sciences, Beijing 100049, P. R. China.
Electronic Supplementary Information (ESI) available: [details of the CV measurement, GPC results, TGA figure, DFT Calculation, charge mobilities and XRD data]. See DOI: 10.1039/x0xx00000x

example, polymer PBDTTBTT exhibited much higher V_{oc} (0.84 V) than alkoxy-substituted PBDTTBTT (0.40 V) in agreement with the increased LUMO levels.[34] Moreover, an alkoxy-substituted PNDI-T2 possessed much higher LUMO level (-3.79 V) than unsubstituted PNDI-T2 (-3.84 V).[27] However, this also resulted in high-lying HOMO level (-5.27 V) that limited its application in all-PSCs as polymer acceptor. To the best of our knowledge, there is no report on the NDI-based polymers that fine tune the energy levels with high LUMO levels and suitable band gap, and it is a greatest challenge to further develop such polymer acceptor with high open circuit voltage.

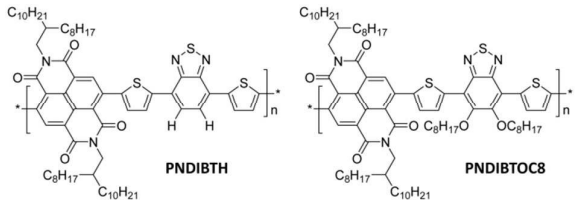

Fig. 1 Chemical structures of polymers PNDIBTH and PNDIBTOC8.

In this contribution, two D-A conjugated polymers, PNDIBTH and PNDIBTOC8, are designed and synthesized by copolymerizing two electron-deficient benzothiadiazole (BT) and NDI units. The unsubstituted-benzothiadiazole (BTH) and its derivative octyloxy-substituted benzothiadiazole (BTOC8) moieties are used as electron-donating units. By contrast research, we have investigated the effect of two alkoxy groups on the photophysical, electronic, as well as the preliminary photovoltaic properties of the new materials in detail. The results reveal that attaching the alkoxy side chain into the NDI-BT based polymer backbones not only allows achieving high molecular weight of PNDIBTOC8, but also fine tunes the energy levels of polymer. To our delight, PNDIBTOC8 exhibits a raised LUMO energy level of -3.72 eV, while the LUMO level of PNDIBTH is located at -3.93 eV. Devices based on PNDIBTOC8 provides high PCE of 3.14% with high V_{oc} of 0.90 V in all-PSCs when blended with PBDTTT-C-T[35] as donor material, which is much higher than that of the PNDIBTH-based device (PCE of 1.20% with V_{oc} of 0.76 V). Notably, high V_{oc} of 0.90 V is among the highest values for NDI-based copolymer recorded in all-PSCs. The atom force microscopy (AFM) and transmission electron microscopy (TEM) measurements reveal the clear correlations of the film morphology with the charge mobilities and performance of all-PSCs.

Experimental section

Materials and Instruments

Compound N,N'-bis(2-octyldodecyl)-2,6-dibromo-1,4,5,8-naphthalene diimide (1), N,N'-bis(2-octyldodecyl)-2,6-bis([2,2']-bithiophenyl-5-yl)-1,4,5,8-naphthalene Diimide (2) and N,N'-bis(2-octyldodecyl)-2,6-bis(5-bromo-thiophenyl-5-yl)-1,4,5,8-naphthalene Diimide (3) were synthesized according to our previous work.[23,37] Compounds 4,7-dibromo-5,6-bis(octyloxy)benzo[1,2,5]thiadiazole (4) was purchased from Innochem (Beijing) Technology Co. Ltd. The donor PBDTTT-C-T were purchased from Solarmer Materials Inc. and used as received. The number-average molecular weight (M_n) and polydispersity index (PDI) of PBDTTT-C-T provided on the Certificate of Analysis were 54.9 kg mol^{-1} and 1.9, respectively. Toluene was dried over Na/benzophenoneketyl and freshly distilled before use. The other reagents and solvents used in this work were commercially purchased and used without further purification. All reactions and manipulations were carried out under argon atmosphere and the column purification of compounds was performed on silica gel.

^{1}H NMR spectra and ^{13}C NMR spectra were performed on a Bruker DMX-400 spectrometer in CDCl3 (^{1}H, δ: 7.26 ppm; ^{13}C, δ: 77 ppm), and high resolution mass spectra were performed on Bruker Autoflex III mass spectrometer. Gel permeation chromatography (GPC) analysis was recorded using Polymer Laboratories PL 220 using 1,2,4-tricholorobenzene (TCB) as eluent at 150 °C. The obtained molecular weight is calibrated with the polystyrene standard. Thermal gravity analyses (TGA) were conducted with a TA Instrument NETZSCH STA 409 PC/PG analyzer operated at a heating rate of 10 °C/min under nitrogen atmosphere. Cyclic voltammetry measurements were done on a Zahner IM6e electrochemical workstation with a three-electrode system in a solution of 0.1 M Bu_4NPF_6 in anhydrous acetonitrile at a scan rate of 50 mV/s. UV-visible (UV-vis) absorption spectra were taken on a Shimidazu UV-3600 UV-vis spectrophotometer in dichlorobenzene solution or as film on quartz. Polymer thin films were prepared from 3.0 mg/mL solution in DCB and the thickness is about 30 nm. The surface morphology of the layers was determined by atomic-force microscopy (AFM, Digital Instruments Nano Scope III) with tapping model. Transmission electron microscopy (TEM) images were taken on a JEM-2100 transmission electron microscope operated at an acceleration voltage of 200 kV. The samples used in AFM and TEM measurement are from the naked active layer of devices. The thickness of the functional layers was measured using a KLA-T encore P-6 profilometer (Tencor).

Synthesis of Monomers and Polymers

5,6-bis(octyloxy)-4,7-di(thiophen-2-yl)benzo[c][1,2,5] thiadiazole (5). Compound 4 (5.00 g, 9.13 mmol), $Pd(PPh_3)_2Cl_2$ (0.64 g, 0.913 mmol) were added into a 100 mL round-bottom flask. The flask was purged with argon before adding 50 mL of toluene as a solvent. Afterward, 2-(tributylstannyl)thiophene (3.75 g, 10.04 mol) was added. After stirring the mixture overnight at 110 °C, the reaction was quenched by adding CaF_2•$12H_2O$. After removing the solvent under vacuum, the mixed solid was resolved in ethyl acetate, and extracted with water (2×100 mL). The combined organic layer was washed well with brine solution and then dried over anhydeous Na_2SO_4. The solvent was removed by rotary evaporation and the crude product was purified by column flash chromatography using petroleum ether. The pure product was obtained as a yellow power (4.93 g, yield 97%). ^{1}H NMR (400 MHz, $CDCl_3$, δ (ppm)): 8.47 (d, J = 4 Hz, 2H), 7.50 (d, J = 4 Hz, 2H), 7.25 (m, J = 3 Hz, 2H), 4.11 (t, J = 8 Hz, 4H), 1.92(m, 4H), 1.40-1.20 (m, 20H), 0.90

(t, *J* = 8 Hz, 6H); ^{13}C NMR (300 MHz, $CDCl_3$, δ (ppm)): 151.99, 151.02, 134.13, 130.55, 127.31, 126.76, 117.64, 74.38, 31.84, 30.35, 29.52, 29.29, 25.97, 22.68, 14.12; MS (MALDL): m/z 556.8 (M^+).

5,6-bis(octyloxy)-4,7-bis(5-(tributhylstannyl)thiophen-2-yl) benzo[c][1,2,5]thiadiazole (6). Compound 4 (1.00 g, 1.80 mmol) was added into a 100 mL round-bottom flask. Afterwards, 25 mL of THF was added under argon atmosphere. The mixture was cooled to -78 °C in a low-temperature reactor and 1.0 M LDA solution in THF (3.96 mL, 3.96 mmol) was added dropwise. After stirring the mixture for one hour at -78 °C, 1 M tributhyltinchloride solution in THF (4.20 mL, 4.14 mmol) was added in one portion at -78 °C. The mixture was warmed up to room temperature in 60 min. After stirring overnight at room temperature, the solvent was evaporated by using a vacuum rotary evaporator. After reprecipitation in MeOH, a yellow solid was obtained and subsequently used in polymerization without further purification (0.67 g; yield 42 %). ^{1}H NMR ($CDCl_3$, 300 MHz, δ (ppm)): 8.43 (d, *J* = 3.5 Hz, 2H), 7.24 (d, *J* = 3.5 Hz, 2H), 4.03 (t, *J* = 6.9 Hz, 4H),1.91-1.76 (m, 4H), 1.20 (d, *J* = 15.1, 4.2 Hz, 24H), 0.81 (d, *J* = 6.9 Hz, 6H), 0.51-0.21 (m, 18H); ^{13}C NMR (300 MHz, $CDCl_3$, δ (ppm)): 152.09, 151.92, 151.29, 140.34, 139.83, 134.84, 131.33, 117.73, 74.35, 31.86, 30.41, 29.59, 29.29, 26.06, 22.69, 14.12; MS (MALDL): m/z 1136.0 (M^+).

Preperation of poly[N,N′-bis(2-octyldodecyl)-2,6-bis-([2,2′]-bithiophenyl-5-yl)-1,4,5,8-naphthalene diimide-2,2′-diyl]-alt-4,7-(2,1,3-benzothiadiazole) (PNDIBTH). Compound 3 (197 mg, 0.15 mmol), 4,7-bis(boronic acid pinacol ester)-2,1,3-benzothiadiazole (58 mg, 0.15 mmol), $Pd(PPh_3)_4$ (18 mg, 0.15 mol), one drop of Aliquat 336, 2 M aqueous K_2CO_3 solution (3 mL) and 3 mL toluene were added to a Schlenk tube. The tube was purged with argon through a freeze-pump-thaw cycle for three times. The mixture was stirred for 3 days at 110 °C. Then a toluene solution of phenyl boronic acid was added and the mixture was stried for an additional of 6 h, followed by the addition of a few drops of bromobenzene, and then stried for another 6h. The mixture was cooled to room temperature and precipitated into methanol (200 mL). The precipitate was filtered off and purified via Soxhlet extraction for 12 h with methanol, acetone, hexane, choloroform, chlorobenzene and finally collected with dichlorobenzene. The dichlorobenzene solution was then concentrated by evaporation, precipitated into methanol (200 mL), and filtered off to afford a dark blue solid (61 mg, yield 47%).

Preperation of poly[N,N′-bis(2-octyldodecyl)-2,6-bis(thiophenyl-5-yl)-1,4,5,8-naphthalene diimide-2,2′-diyl]-alt-4,7-(5′,6′-bis(hexyloxy)-2,1,3-benzothiadiazole)] (PNDIBTOC8). Compound 1 (984.5 mg, 1.0 mmol), compound 6 (909.0 mg, 1.03 mmol), $Pd_2(dba)_3$ (91.6 mg, 0.1 mmol), P(*o*-tol)$_3$ (121.7 mg, 0.4 mmol) and 6 mL of toluene were added to a Schlenk tube. The tube was charged with nitrogen through a freeze-pump-thaw cycle for three times. The mixture was stirred for 48 h at 110 °C. Then a toluene solution of 2-(tributylstannyl)thiophene was added and the mixture was stirred for an additional of 6 h, followed by the addition of a few drops of bromobenzene, and then stirred for another 6h. The mixture was cooled to room temperature and precipitated into methanol (100 mL). The precipitate was filtered through a nylon filter, purified via Soxhlet extraction for 12 h with methanol, acetone, hexane, and finally collected with chloroform. The chloroform solution was then concentrated by evaporation, precipitated into methanol (100 mL), and filtered off to afford a dark blue solid (77.5 mg, yield 72%).

Fabrication and Characterization of PSCs

The PSC devices were fabricated with a structure of ITO/PEDOT:PSS/active layer/Ca/Al. Patterned ITO-glass substrates were used as the anode in polymer solar cells. ITO substrates were firstly pre-cleaned sequentially by sonicating in a detergent bath, de-ionized water, acetone, and isopropanol each for 20 min, and then dried in an oven for 30 min, which were then subjected to a UV/ozone treatment for 60 min. A thin layer of PEDOT:PSS (poly(3,4ethylenedioxythiophene):poly(styrenesulfonate)) was spin-casted onto the ITO surface. After being baked at 150 °C for 20 min in ambient air, the substrates were transferred into a nitrogen-filled glove box (<0.1 ppm O_2 and H_2O). PNDIBTH or PNDIBTOC8 was blended with donor PBDTTT-C-T and dissolved in 1,2-dichlorobenzene (*o*-DCB). Subsequently, the active layers were spin-casted from solutions (20 mg/mL, polymer weight concentration) with various rotational speeds on the ITO/PEDOT:PSS substrates. A small amount of DIO was added into the polymer solution as an additive to optimize the photovoltaic performance of the devices if necessary. Beside this, no further treatment to the blend film was performed before the deposition of the metal electrode. Finally, a Ca/Al metal top electrode was deposited under vacuum onto the active layer at a pressure of ca. 1.0×10^{-4} Pa. The active area of the device was 6.0 mm^2 defined by shadow masks. The current density-voltage (J-V) characteristics were measured by a computer-controlled Keithley 2400 Source Measure Unit. The photocurrent was measured under an AM 1.5 solar spectrum filter, calibrated with a standard Si solar cell and the optical power was 100 mW cm^{-2}. The EQE measurements of the encapsulated devices were performed in air (PV Measurements Inc., Model QEX7). The hole and electron mobilities were calculated by fitting the dark *J-V* curves for the hole-only and electron-only devices to the space-charge limited current (SCLC) model at low voltages.

Results and discussion

Synthesis and characterization

The synthesis of PNDIBTH and PNDIBTOC8 is depicted in Scheme 1. Polymer PNDIBTH was synthesized by Suzuki coupling reaction between N,N'-bis (2-octyldodecyl)-2,6-bis(5-bromo-thiophenyl-5-yl)-1,4,5,8-naphthalene diimide (monomer 3) and 4,7-bis(boronic acid pinacol ester)-2,1,3-benzothiadiazole. By Stille coupling copolymerization of N,N'-bis(2-octyldodecyl)-2,6-dibromo-1,4,5,8-naphthalene diimide and 5,6-bis(octyloxy)-4,7-bis(5-(tributylstannyl)thiophen-2-yl) benzo[1,2,5]thiadiazole, polymer PNDIBTOC8 was synthesized.

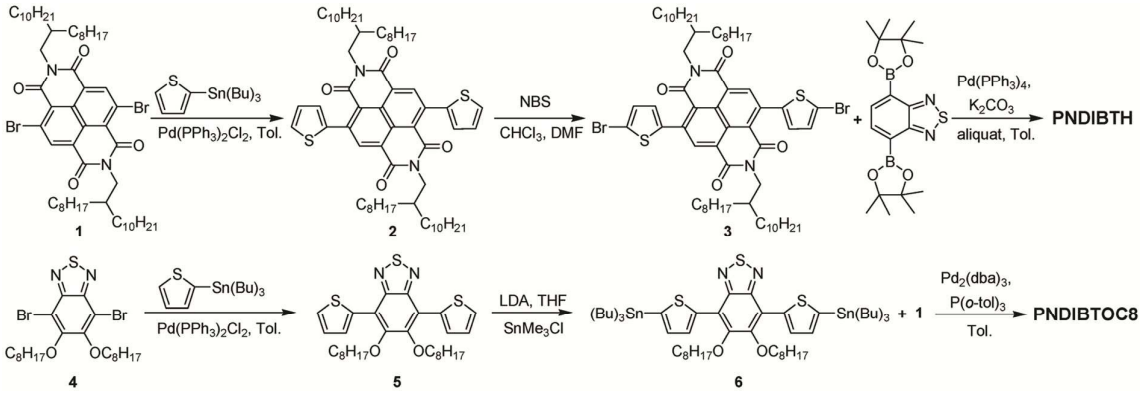

Scheme 1. Synthetic route to monomers and polymers PNDIBTH and PNDIBTOC8.

Table 1 Polymerization results and thermal, optical and electrochemical properities of polymers PNDIBTH and PNDIBTOC8

Polymer	M_n [a] (kPa)	PDI[a]	T_d [b] (°C)	λ_{max} [c] (nm) solution	λ_{max} [d] (nm) film	E_g^{opt} [e](eV)	E_{LUMO} [f](eV)	E_{HOMO} [f] (eV)	E_g^{cv} [g] (eV)	E_g^{DFT} [h](eV)
PNDIBTH	24.1	1.9	432	364, 709	366, 666, 717	1.55	-3.93	-5.94	2.01	1.85
PNDIBTOC8	66.7	2.2	343	346, 674	362, 680	1.46	-3.72	-5.82	2.10	1.91

[a] Weight average molecular weight (M_n) and polydispersities (PDI) of the polymers were determined by GPC using polystyrene standards. [b] Decomposition temperature, determined by TGA in nitrogen at a heating rate of 10 °C min^{-1}, based on 5% weight loss. [c] Measurements in dichlorobenzene solution. [d] Measurements in thin film were performed on the glass substrate. [e] Band gap estimated from the onset wavelength of the optical absorption in thin film. [f] The HOMO and LUMO levels were estimated from cyclic voltammetry analysis. [g] The electrochemical band gap values estimated from the HOMO and LUMO values. [h] The calculated band gap values estimated from DFT calculations (B3LYP/6-31G(d)).

The obtained polymers were precipitated in methanol and then purified by Soxhlet extraction to remove oligomers and other impurities. PNDIBTH possesses poor solubility, and is only soluble in hot dichlorobenzene. In contrast, PNDIBTOC8 is well soluble in common organic solvents due to the solubilization of alkoxy side chain, allowing us to achieve high number-average-molecular weights (M_n). Molecule weights of two polymers were evaluated by high temperature gel permeation chromatography (GPC) eluted with 1,2,4-trichlorobenzene at 150 °C. PNDIBTOC8 (66.7 kDa) showed a higher M_n than PNDIBTH (23.0 kDa) as well as slightly larger polydispersity index (PDI: 2.2 vs 1.9). The lower molecule weight of PNDIBTH is probably due to its poor solubility in the reaction solvent of toluene. Thermogravimetric analysis suggests that polymers have excellent thermal stability up to 432 °C for PNDIBTH and 343 °C for PNDIBTOC8 with 5% weight loss under N_2 atmosphere (Fig. S2).

Optical and electrochemical properities

The normalized UV-vis absorption spectra of PNDIBTH and PNDIBTOC8 in dilute dichlorobenzene solution (ca. 10^{-6} M) and thin film are showed in Fig.2. The detailed absorption data and the optical band gap deduced from the absorption edge in films are collected and listed in Table 1. The two polymers show very similar absorption in dilute solution with major absorption peak at 709 nm for PNDIBTH and 674 nm for PNDIBTOC8. After incorporating the two alkoxy groups into the backbone of polymer, an obvious blue shift occurs toward

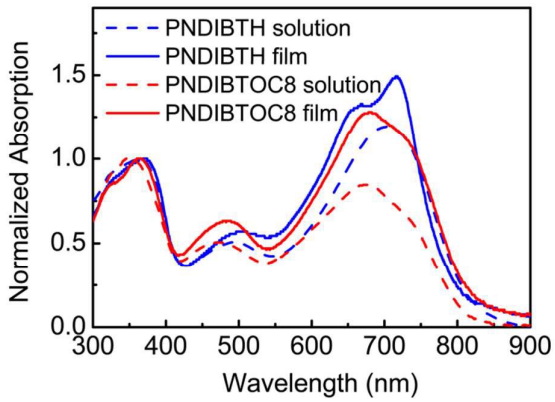

Fig. 2 Absorption spectra of polymers PNDIBTH and PNDIBTOC8 in toluene and as thin film.

short-wavelength. This typical band can be assigned to the intramolecular charge transfer (ICT) interactions between the electron-donating and electron-deficient units. The other band in short-wavelength around 350 nm can be assigned to the π-π* transition of 4,7-dithien-2,1,3-benzothiazdiazole (DTBT) unit or 5,6-bis(octyloxy)-4,7-dithien-2,1,3-benzothiazdiazole (DTBTOC8) units.[36] In solid state, the absorption of PNDIBTH, including the 0-0 vibrational peak at 666 nm and the 0-1 vibrational peak at 717 nm, shows obviously red shifts compared with that in solution, which are attributed to solid-state packing effects. In contrast, PNDIBTOC8 in film exhibits a

broad peak and a small red shift by 6 nm relative to that in solution, which demonstrates that the backbone of PNDIBTOC8 might become less coplanar due to the existence of two alkoxy chains. Moreover, PNDIBTOC8 shows a optical energy gap of 1.46 eV, much smaller than that of PNDIBTH (1.55 eV), which mainly contributes to the high molecular weight of PNDIBTOC8.

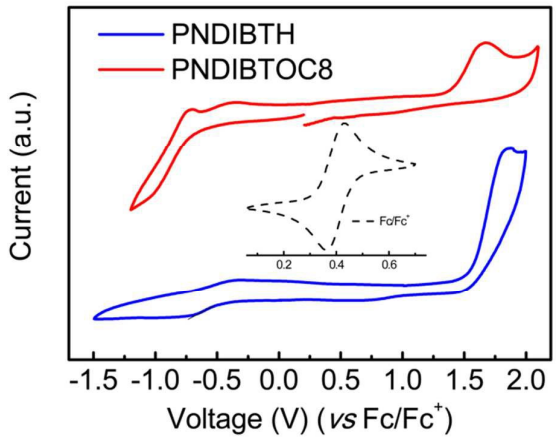

Fig. 3 Cyclic viltammograms of polymers PNDIBTH and PNDIBTOC8 films cast on a platinum working electrode in 0.1M TBATFB/acetontrile at 50 mV s^{-1}, potential vs.Fe/Fe^{+}.

HOMO and LUMO energy levels of two polymers were estimated from their onset oxidation potential (E_{ox}) and onset reduction potential (E_{red}) as determined by cyclic voltammetry on drop-cast polymer films, and listed in Table 1. The cyclic voltammograms of the polymers are showed in Fig.3. From the values of E_{ox}/E_{red} of polymers, the LUMO/HOMO values (vs. vacuum) of polymers were -3.93/-5.94 eV for PNDIBTH and -3.72/-5.82 eV for PNDIBTOC8. It is obvious that introduction of the alkoxy group can effectively raise the LUMO/HOMO energy levels of PNDIBTOC8, which is contributed to the electron-donating property of alkoxy group. Moreover, the band gap of PNDIBTH and PNDIBTOC8 were estimated to be 2.01 and 2.10 eV, respectively. This trend is also consistent with our quantum-chemical calculation results (see Table 1). In order to reduce the calculation time, long alkyl chains were replaced by methyl groups in the calculations. As showed in Fig.S3 and Table S1, trimer of NDIBTOC8 possesses much higher LUMO/HOMO energy levels and larger band gap than that of trimer of NDIBTH. Additionally, PNDIBTOC8 exhibits much high-lying LUMO level of -3.72 eV, which enables a high V_{oc} when blended with PBDTTT-C-T as donor material. The LUMO-LUMO offset of PBDTTT-C-T and PNDIBTOC8 is larger than 0.35 eV, which offers reasonable driving force for charge generation. In the view of energy levels of donor and acceptor, PNDIBTOC8 holds promise as an alternative material for fullerene derivatives.

Photovoltaic properties

Solution-processed BHJ device were fabricated using the resulting polymers as electron acceptor with a conventional device structure of ITO/PEDOT:PSS/PBDTTT-C-T:polymer/Ca/Al. PBDTTT-C-T was a typical polymer used as electron donor.[35] The photoactive layers were obtained by spin casting the PBDTTT-C-T:polymer blends from DCB or DCB:DIO solution without any other treatment. The measurements were performed under simulated AM1.5G, 100 mW cm^{-2} illumination with an active area of 0.06 cm^2. The current density-voltage (J-V) characteristics of these PSCs are showed in Fig.4 and the device parameters such as V_{oc}, short-circuit current (J_{sc}), fill factor (FF) and PCE are summarized in Table 2. The donor:acceptor (D:A) ratio plays an important role in the performance of PSCs because a balance in the hole and electron transport is necessary to avoid any accumulation of charge and thus to facilitate the charge transport process. Therefore, the blending ratio of PNDIBTOC8 in active layer was changed from 20 to 60 wt% to optimize the device performance (Table 2). It is noted that V_{oc} decreases slightly with increasing the content of PNDIBTOC8 in blend film, about 0.90 V. As we expected, the devices from PNDIBTOC8 show a high V_{oc}, which comes from with the raised LUMO level of PNDIBTOC8. To the best of our knowledge, the high V_{oc} of 0.90 V is among the highest values for NDI-based copolymer recorded in all-PSCS. Except V_{oc}, the other photovoltaic parameters strongly depended on the D:A ratio. The values of J_{sc} increased from 3.73 to 5.34 mA cm^{-2} when the PNDIBTOC8 content was increased from 20 to 50 wt%, and it decreased slightly at 60 wt%. The FF decreased from 45.7% to 40.8% with increasing PNDIBTOC8 content and the highest value was obtained for the devices with 20 wt%. A moderate PCE of 2.07%

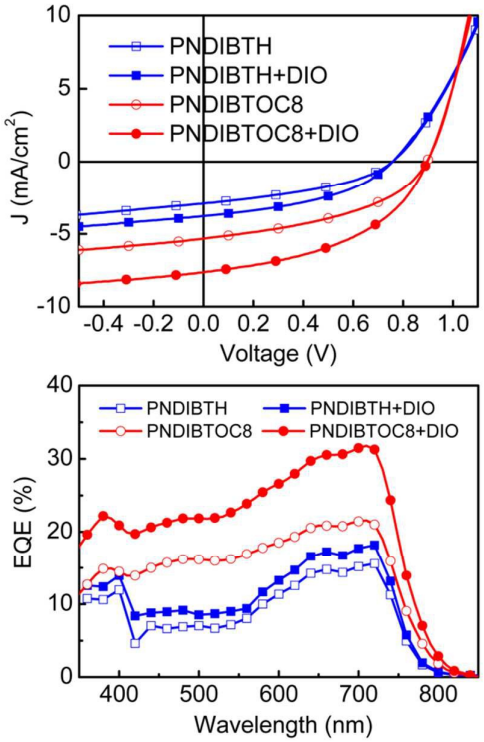

Fig. 4 J-V characteristics and EQE curves of PSCs prepared with the devices structure of ITO/PEDOT:PSS/PBDTTT-C-T:polymer/Ca/Al.

was obtained for the devices with weight ratio of PBDTTT-C-T:PNDIBTOC8 = 60:40. The marked dependence of the PCE suggests the importance of controlling the D:A blending ratio during the fabrication of all-polymer bulk heterojunction solar cells. In addition, the PCE was optimized at a donor rich blend ratio, which is contrast with that reported for polymer/fullerene BHJ solar cells. In order to further improve the performance of devices, a small amount of 1,8-diiodooctane (DIO) was used as additive. The best PCE values of the PSC devices were obtained with 1% DIO as additive. The optimized PCE was 3.14% with photovoltaic parameters J_{sc} of 5.34 mA cm^{-2}, V_{oc} of 0.90 V, FF of 45.6%. However, the device based on PNDIBTH (blend ratio 50:50) gave the best PCE of 0.86% with a moderate V_{oc} of 0.76 V, and showed an improved performance up to 1.20% with DIO as additive, which were both much lower than that of optimized devices based on PNDIBTOC8. Fig.4 shows the current density-voltage (*J*-*V*) characteristic and external quantum efficiency (EQE) spectra of the solar cells based on PNDIBTH (50:50) and PNDIBTOC8 (60:40) blends films processed with or without 1% DIO. The photorespones of the devices based on the two polymers extended from 350 nm to 800 nm. The EQE approached a maximum value of 33% at 710 nm for PNDIBTOC8 and 18% at 720 nm for PNDIBTH. This result is consistent with the higher J_{sc} for the PNDIBTOC8 compared to that of PNDIBTH. Moreover, to gain insight into the enhanced performance of devices based on PNDIBTOC8 compared with PNDIBTH, the mobility of the blend films were measured by the space-charge limited current (SCLC) method (Fig. S4). The hole and electron mobilities of devices based on polymer were 1.8×10^{-4} and 9.4×10^{-5} cm^2 V^{-1} s^{-1} for PNDIBTH, 4.2×10^{-4} and 2.8×10^{-4} cm^2 V^{-1} s^{-1} for PNDIBOC8, respectively. The balanced and increased

Table 2 PSCs performances of devices based on polymers PNDIBTH and PNDIBTOC8 as acceptor

Polymer:Donor (weight ratio)	V_{oc} (V)[a]	J_{sc} (mA/cm^2)[b]	FF (%)[c]	PCE (%)[d]
PNDIBTH:Donor(40:60)	0.72 ±0.01	2.00±0.24	38.8± 0.32	0.55± 0.08
PNDIBTH:Donor(50:50)	0.76 ±0.01	2.90±0.05	39.5±0.40	0.86± 0.14
PNDIBTH:Donor(60:40)	0.76±0.02	2.66±0.13	40.3±0.43	0.81±0.05
PNDIBTH:Donor(70:30)	0.74±0.03	2.30±0.28	43.1±0.51	0.73±0.16
PNDIBTH:Donor(50:50) with 1% DIO	0.76 ±0.01	3.77±0.15	42.0± 0.36	1.20± 0.11
PNDIBTOC8:Donor(20:80)	0.92 ±0.02	3.73±0.22	45.7± 0.13	1.57± 0.10
PNDIBTOC8:Donor(30:70)	0.90 ±0.02	5.11±0.17	44.5±0.19	2.05± 0.21
PNDIBTOC8:Donor(40:60)	0.89 ±0.01	5.23±0.10	43.7±0.23	2.07± 0.05
PNDIBTOC8:Donor(50:50)	0.89 ±0.01	5.34±0.21	41.1±0.30	1.95± 0.10
PNDIBTOC8:Donor(60:40)	0.88 ±0.02	4.00±0.08	40.8±0.14	1.44±0.18
PNDIBTOC8:Donor(40:60) with 1% DIO	0.90 ±0.01	7.65±0.13	45.6±0.22	3.14± 0.13

[a] Open-circuit voltage. [b] Short-circuit current density. [c] Fill factor. d Power conversion efficiency (averages of 5 PSC devices are reported for each blend).

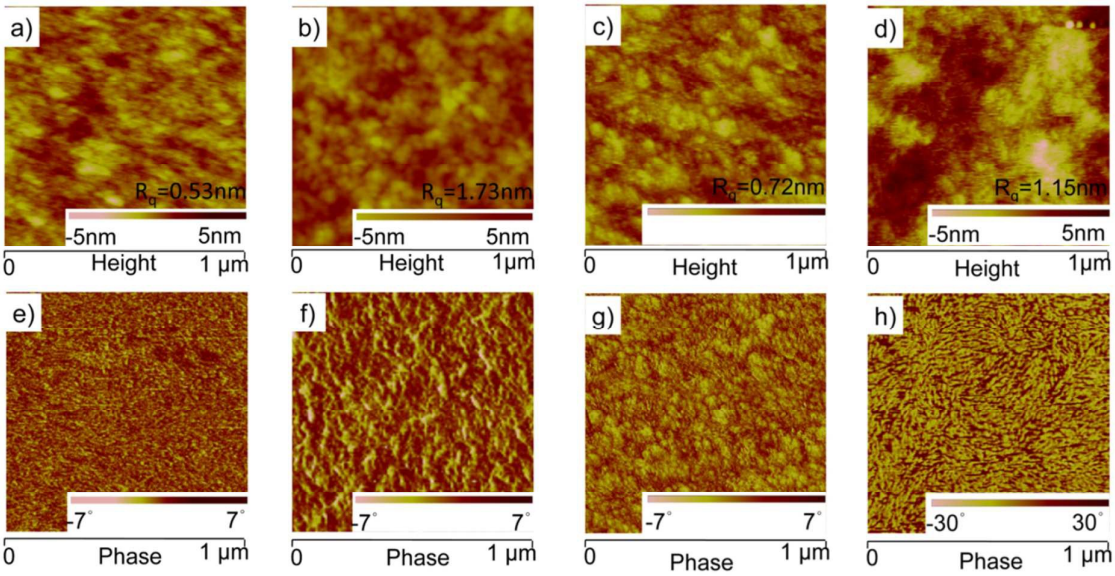

Fig. 5 AFM images of the blend films of PNDIBTH:PBDTTT-C-T (50:50 wt%) (images a, b, e and f) and PNDIBTOC8:PBDTTT-C-T(60:40 wt%) (images c, d, g and h) without DIO (images a, c, e and g) and with 1% DIO (images b, d, f and h).

hole and electron mobilities of donor:PNDIBTOC8 blend films can largely explain the enhanced photovoltaic parameters in terms of J_{sc}, FF and the high PCE value of all-polymer solar cell.

Morphology

To explode the reasons for the improved device performance of polymer PNDIBTH and PNDIBTOC8, atomic force microscopy (AFM) and transmission electron microscopy (TEM) images of the PBDTTT-C-T:polymer blend films were recorded and displayed in Fig. 4 and Fig.6. In Fig.5a and c, the blend films of PNDIBTH and PNDIBTOC8 showed a small root-mean-square (RMS) of 0.75 and 0.72 nm with weak phase separation, which is not ideal for efficient charge dissociation. Using DIO for additive yields blend films of two polymers exhibiting enhanced phase separation with larger RMS values, 1.73 nm for PNDIBTH and 1.15 nm for PNDIBTOC8. For PNDIBTOC8, blend film processed with 1% DIO showed a favourable phase-separated surface morphology with domain size of about 10-30 nm (Fig. 4h). The much fine domain sizes and more continuous interpenetrating structure in blend film demonstrates that the surface morphology of the all-polymer blend solar cells is successfully varied by adding small amount of DIO. Such a large difference of surface morphology is expected to translate the differences in charge separation at D:A interfaces and charge transport in blends. Therefore, these results are attributed to the significantly improved J_{sc} and FF after treatment with DIO. Moreover, the TEM analysis was employed to provide more direct observation of phase separation of blend films based on PNDIBTOC8 and PNDIBTH. Fig.6 showed distinctly different phase separation of blend films based on PNDIBTH and PNDIBTOC8. The blend film of PNDIBTH exhibits obscure domains without clear phase segregation. In contrast, the PBDTTT-C-T:PNDIBTOC8 blend film showed dendrite-like continuous phase separation, which can not only enlarge the D/A interfacial areas to benefit the exiton separation and free charge generation, but also afford the charge transport channel. The special phase separation for PNDIBTOC8 can largely explain the enhanced photovoltaic parameters in terms of J_{sc}, FF and thus the high PCE value of all-polymer solar cells.

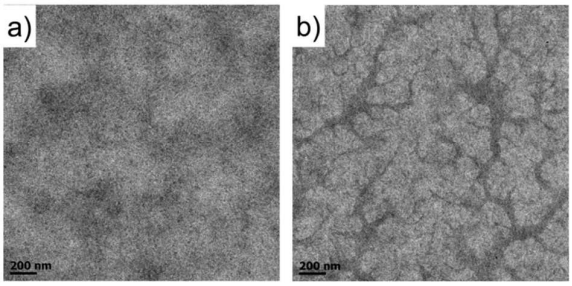

Fig 6 TEM images of the blend films of PNDIBTH:PBDTTT-C-T (50:50 wt%) (a) and PNDIBTOC8:PBDTTT-C-T(60:40 wt%) (b) with 1% DIO.

Conclusions

In summary, two polymer acceptors based on NDI unit copolymerized with electron-deficient BTH and BTOC8 units were designed and synthesized. Incorporating octyloxy side chain into the benzothiadiazole in PNDIBTOC8 can not only greatly increase the solubility, but also elevate the LUMO levels to -3.72 V and maintain a medium bandgap of 2.10 eV. All-polymer photovoltaic devices based on PNDIBTOC8 achieve the high power conversion efficiency of 3.14% with high V_{oc} of 0.90 V, which is higher than that of PNDIBTH-based device (PCE of 1.20% with V_{oc} of 0.76 V). The high open-circuit voltage is attributed to the raised LUMO level of PNDIBTOC8, and this value is among the highest V_{oc} value for NDI-based copolymer recorded in all-PSCs. The TEM imges revealed that blend film of PBDTTT-C-T:PNDIBTOC8 showed dendrite-like continuous phase separation contributed to the high and more-balanced hole and electron mobilities. Further, these results represent a successful example of fine tuning the energy levels of acceptor to obtain high open circuit voltage and excellent performance for all-PSCs.

Acknowledgements

This work was supported by the National Natural Science Foundation of China (No. 21073200, 21273251, 91333111, 21190034, 21221002, 21373239 and 21203212), the Beijing Municipal Science & Technology Commission (No. Z131103002813097), the project of Construction of Innovative Teams and Teacher Career Development for Universities and Colleges Under Beijing Municipality (IDHT20140512), the National Basic Research Program of China (973) (2011CB808402, 2013CB933500).

Notes and references

1 A. J. Heeger, *Adv. Mater.*, 2014, **26**, 10-28.
2 L. Gang; Z. Rui and Y. Yang, *Nat. Photon.*, 2012, **6**, 153-161.
3 Y. Lin; Y. Li and X. Zhan, *Chem. Soc. Rev.*, 2012, **41**, 4245-4272.
4 S. Günes; H. Neugebauer and N. S. Sariciftci, *Chem. Rev.*, 2007, **107**, 1324-1338.
5 V. Vohra; K. Kawashima; T. Kakara; T. Koganezawa; I. Osaka; K. Takimiya; H. Murata, *Nat. Photon.,* 2015, **9**, 403-408.
6 Q. Zhang; B. Kan; F. Liu; G. Long; X. Wan; X. Chen; Y. Zuo; W. Ni; H. Zhang; M. Li; Z. Hu; F. Huang; Y. Cao; Z. Liang; M. Zhang; T. P. Russell and Y. Chen, *Nat. Photon.*, 2014, **9**, 35-41.
7 C. Z. Zhicai He, Shijian Su, Miao Xu, Hongbin Wu and Yong Cao, *Nat. Photon.*, 2012, **6**, 593-597.
8 X. Guo; N. Zhou; S. J. Lou; J. Smith; D. B. Tice; J. W. Hennek; R. P. Ortiz; J. T. L. Navarrete; S. Li; J. Strzalka; L. X. Chen; R. P. H. Chang; A. Facchetti and T. J. Marks, *Nat. Photon.*, 2013, **7**, 825-833.
9 N. Zhou; X. Guo; R. P. Ortiz; S. Li; S. Zhang; R. P. H. Chang; A. Facchetti and T. J. Marks, *Adv. Mater.*, 2012, **24**, 2242-2248.
10 J. E. Anthony, *Chem. Mater.*, 2010, **23**, 583-590.
11 J. D. Servaites; B. M. Savoie; J. B. Brink; T. J. Marks and M. A. Ratner, *Energ. Environ. Sci.*, 2012, **5**, 8343-8350.
12 A. Facchetti, *Mater. Today*, 2013, **16**, 123-132.
13 P. E. Hartnett; A. Timalsina; H. S. S. R. Matte; N. Zhou; X. Guo; W. Zhao; A. Facchetti; R. P. H. Chang; M. C. Hersam; M.

R. Wasielewski and T. J. Marks, *J. Am. Chem. Soc.*, 2014, **136**, 16345-16356.
14 T. Earmme; Y.-J. Hwang; N. M. Murari; S. Subramaniyan and S. A. Jenekhe, *J. Am. Chem. Soc.*, 2013, **135**, 14960-14963.
15 T. Earmme; Y.-J. Hwang; S. Subramaniyan and S. A. Jenekhe, *Adv. Mater.*, 2014, **26**, 6080-6085.
16 D. Mori; H. Benten; I. Okada; H. Ohkita and S. Ito, *Energ. Environ. Sci.*, 2014, **7**, 2939-2943.
17 Y. Zhou; T. Kurosawa; W. Ma; Y. Guo; L. Fang; K. Vandewal; Y. Diao; C. Wang; Q. Yan; J. Reinspach; J. Mei; A. L. Appleton; G. I. Koleilat; Y. Gao; S. C. B. Mannsfeld; A. Salleo; H. Ade; D. Zhao and Z. Bao, *Adv. Mater.*, 2014, **26**, 3767-3772.
18 Y.-J. HouHwang; T. Earmme; B. A. E. Courtright; F. N. Eberle and S. A. Jenekhe, *J. Am. Chem. Soc.*, 2015, **137**, 4424-4434.
19 C. Lee; H. Kang; W. Lee; T. Kim; K.-H. Kim; H. Y. Woo; C. Wang and B. J. Kim, *Adv. Mater.*, 2015, **27**, 2466-2471.
20 S. Subramaniyan; T. Earmme; N. M. Murari and S. A. Jenekhe, *Polym. Chem.*, 2014, **5**, 5707-5715.
21 E. Zhou; J. Cong; K. Hashimoto and K. Tajima, *Adv. Mater.*, 2013, **25**, 6991-6996.
22 H. Yan; Z. Chen; Y. Zheng; C. Newman; J. R. Quinn; F. Dotz; M. Kastler and A. Facchetti, *Nature*, 2009, **457**, 679-686.
23 C. Gu; W. Hu; J. Yao and H. Fu, *Chem. Mater.*, 2013, **25**, 2178-2183.
24 24 H. Chen; Y. Guo; Z. Mao; G. Yu; J. Huang; Y. Zhao and Y. Liu, *Chem. Mater.*, 2013, **25**, 3589-3596.
25 Y.-J. Hwang; G. Ren; N. M. Murari and S. A. Jenekhe, *Macromolecules*, 2012, **45**, 9056-9062.
26 Y. Kim; J. Hong; J. H. Oh and C. Yang, *Chem. Mater.*, 2013, **25**, 3251-3259.
27 27 X. Guo; F. S. Kim; M. J. Seger; S. A. Jenekhe and M. D. Watson, *Chem. Mater.*, 2012, **24**, 1434-1442.
28 M. Schubert; D. Dolfen; J. Frisch; S. Roland; R. Steyrleuthner; B. Stiller; Z. Chen; U. Scherf; N. Koch; A. Facchetti and D. Neher, *Adv. Energy Mater.*, 2012, **2**, 369-380.
29 D. Mori; H. Benten; I. Okada; H. Ohkita and S. Ito, *Adv. Energy Mater.*, 2014, **4**, 1301006-1301012.
30 S. Yum; T. K. An; X. Wang; W. Lee; M. A. Uddin; Y. J. Kim; T. L. Nguyen; S. Xu; S. Hwang; C. E. Park and H. Y. Woo, *Chem. Mater.*, 2014, **26**, 2147-2154.
31 N. Wang; Z. Chen; W. Wei and Z. Jiang, *J. Am. Chem. Soc.*, 2013, **135**, 17060-17068.
32 H. Li; C. Gu; L. Jiang; L. Wei; W. Hu and H. Fu, *J. Mater. Chem. C*, 2013, **1**, 2021-2027.
33 H. Zhou; L. Yang; A. C. Stuart; S. C. Price; S. Liu and W. You, *Angew. Chem. Int. Ed.*, 2011, **50**, 2995-2998.
34 J. Hou; H.-Y. Chen; S. Zhang and Y. Yang, *J. Phys. Chem. C*, 2009, **113**, 21202-21207.
35 L. Huo; S. Zhang; X. Guo; F. Xu; Y. Li and J. Hou, *Angew. Chem.*, 2011, **123**, 9871-9876.
36 36 R. Steyrleuthner; R. Di Pietro; B. A. Collins; F. Polzer; S. Himmelberger; M. Schubert; Z. Chen; S. Zhang; A. Salleo; H. Ade; A. Facchetti and D. Neher, *J. Am. Chem. Soc.*, 2014, **136**, 4245-4256.
37 X. Guo and M. D. Watson, *Org. Lett.*, 2008, **10**, 5333-5336.